PHYSOR 2004 -The Physics of Fuel Cycles and Advanced Nuclear Systems: Global Developments
Chicago, Illinois, April 25-29, 2004, on CD-ROM, American Nuclear Society, Lagrange Park, IL. (2004)

BN-600 Full MOX Core Benchmark Analysis

Y. I. Kim[*1], R. Hill[2], K. Grimm[2], G. Rimpault[3], T. Newton[4], Z. H. Li[5], A. Rineiski[6], P. Mohanakrishan[7], M. Ishikawa[8], K. B. Lee[9], A. Danilytchev[10] and V. Stogov[10]
[1]*International Atomic Energy Agency (IAEA), Wagramer Strasse 5, A-1400, Vienna, Austria*
[2]*Argonne National Laboratory (ANL), 9700 S. Cass Ave., Argonne, IL 60439, USA*
[3]*CE/Cadarache, F-13108 Saint-Paul-Lez-Durance Cedex, France*
[4]*SERCO Assurance (SA), Dorset DT2 8DH, United Kingdom*
[5]*China Institute of Atomic Energy (CIAE), 102413 Beijing, China*
[6]*Forschnungszentrum Karlsruhe(FZK)/IKET, D-76344 Eggenstein-Leopoldshafen, Germany*
[7]*Indira Gandhi Centre for Atomic Research (IGCAR), Kalpakkam Tamil Nadu 603 102, India*
[8]*Japan Nuclear Cycle Development Institute (JNC), Ibaraki 311-1393, Japan*
[9]*Korea Atomic Energy Research Institute (KAERI), Yusong, Taejon 305-600, Rep. of Korea*
[10]*Institute of Physics and Power Engineering (IPPE), Bondarenko Sq. 1, 249 033 Obninsk, Russia*

As a follow-up of the BN-600 hybrid core benchmark, a full MOX core benchmark was performed within the framework of the IAEA co-ordinated research project. Discrepancies between the values of main reactivity coefficients obtained by the participants for the BN-600 full MOX core benchmark appear to be larger than those in the previous hybrid core benchmarks on traditional core configurations. This arises due to uncertainties in the proper modelling of the axial sodium plenum above the core. It was recognized that the sodium density coefficient strongly depends on the core model configuration of interest (hybrid core vs. fully MOX fuelled core with sodium plenum above the core) in conjunction with the calculation method (diffusion vs. transport theory).

The effects of the discrepancies revealed between the participants' results on the ULOF and UTOP transient behaviours of the BN-600 full MOX core were investigated in simplified transient analyses. Generally the diffusion approximation predicts more benign consequences for the ULOF accident but more hazardous ones for the UTOP accident when compared with the transport theory results. The heterogeneity effect does not have any significant effect on the simulation of the transient. The comparison of the transient analyses results concluded that the fuel Doppler coefficient and the sodium density coefficient are the two most important coefficients in understanding the ULOF transient behaviour. In particular, the uncertainty in evaluating the sodium density coefficient distribution has the largest impact on the description of reactor dynamics. This is because the maximum sodium temperature rise takes place at the top of the core and in the sodium plenum.

KEYWORDS: full MOX core benchmark, sodium plenum, sodium density coefficient, fuel Doppler, UTOP, ULOF, hybrid core

1. Introduction

A benchmark analysis of a BN-600 fully mixed oxide (MOX) fuelled core design with sodium plenum above the core has been performed as an extension to the study of the BN-600 hybrid uranium oxide (UOX)/MOX fuelled core carried out during 1999 – 2001. [1] This work was carried out within the framework of the IAEA sponsored Co-ordinated Research Project (CRP) on "Updated Codes and Methods to Reduce the Calculational Uncertainties of the LMFR Reactivity Effects". [2-4] This benchmark analysis retains the general objective of the CRP which is to validate, verify and improve methodologies and computer codes used for the calculation of reactivity coefficients in fast reactors aiming at enhancing the utilization of plutonium and minor actinides. The scope of the benchmark is to reduce the uncertainties of safety relevant reactor physics parameter calculations of MOX fuelled fast reactors and hence to validate and improve data and methods involved in such analyses.

[*] Corresponding author, Tel. +43-1-2600-22808, FAX +43-1- 2600-29598, E-mail: Young-In.Kim@iaea.org

In previous benchmark analyses of the BN-600 hybrid core that closely conforms to a traditional configuration, the comparative analyses showed that sufficient accuracy is achieved using the diffusion theory approximation, widely applied in fast reactor physics calculations. This finding confirmed the reliability of calculations using standard techniques and computer codes employing the diffusion theory approximation, as used in various countries for their fast reactor development project. It is noteworthy that a substantial spread in the results of the participants exists for several reactivity coefficients, particularly, in non-fuelled and peripheral regions which are characterized by their predominant neutron leakage and power distributions. [5] However, the substantial spread did not have a significant impact on the transient behavior prediction, especially up to the onset of sodium boiling in the ULOF transient analyses. This result highlighted the compensating effects between several reactivity effects in the specific design of the hybrid core mainly loaded with UOX fuel.

With the purpose of investigating a core configuration of full MOX fuel loading, a core model of the BN-600 type reactor, designed to reduce the sodium void effect by installing a sodium plenum above the core, was newly defined for the next benchmark study. The specifications and input data for the benchmark neutronics calculations were prepared by IPPE (Russia). [1] The specifications given for the benchmark describe only a preliminary core model variant and represent only one conceptual approach to BN-600 full MOX core designs.

Nine organizations from nine Technical Working Group for Fast Reactors (TWG-FR) Member States and the IAEA participated in this BN-600 fully MOX fuelled core benchmark analysis. The participants applied their own state-of-the-art basic data, computer codes and methods to the benchmark analysis. Within the scope of these core benchmark analyses, they have validated their efforts to update basic nuclear data, and to improve methodologies and computer codes for calculating safety relevant reactor physics parameters. The results for integral and local reactivity coefficient values obtained by the participants were inter-compared in terms of calculational uncertainty resulting from different data and method approximations along with their effects on the ULOF and UTOP transient behaviours. In addition, results were evaluated in comparison with the results for the hybrid core.

2. Benchmark Description

The input data, including the hexagonal (HEX)-Z calculational model for the BN-600 benchmark calculations, are completely described in the benchmark specification. [1] The calculational model, a 60° sector of the layout of the benchmark core, shown in Fig. 1, corresponds to the 1470 MW_{th} total power BN-600 reactor at the beginning of an equilibrium cycle. In principle, the core layout is the same as that of the hybrid core of BN-600. [5] The core consists of a low enrichment MOX inner zone (LEZ), a middle enrichment MOX zone (MEZ), and a high enrichment MOX zone (HEZ). In addition, there is an internal breeding zone (IBZ) in the central 5.1 cm of the LEZ region. For this benchmark configuration, each enriched zone has a burnup of 2 – 3%, while the internal breeding zone, which contains relatively more ^{238}U, has a burnup of 1.7%. Three control rods (SCRs) and one shim control rod (SHR) are radially interspersed in the LEZ region. Radially, beyond the HEZ outer drive zone are two steel shielding zones (SSA1 and SSA2) followed by a radial reflector zone (REF). The same geometry descriptions for fuel subassemblies (FSAs) and control rods (SCR and SHR) have been retained in a triangular lattice of pitch 9.902 cm, with the same simplifications (60° symmetry and exclusion of automatic compensators) as assumed in the previous benchmark studies.

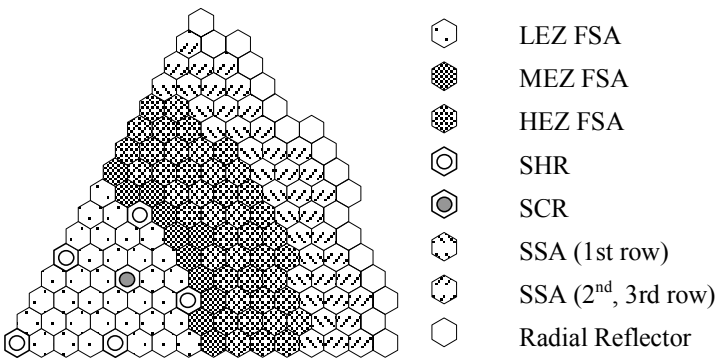

Fig.1 Layout of BN-600 full MOX core model (60° sector, rotational symmetry)

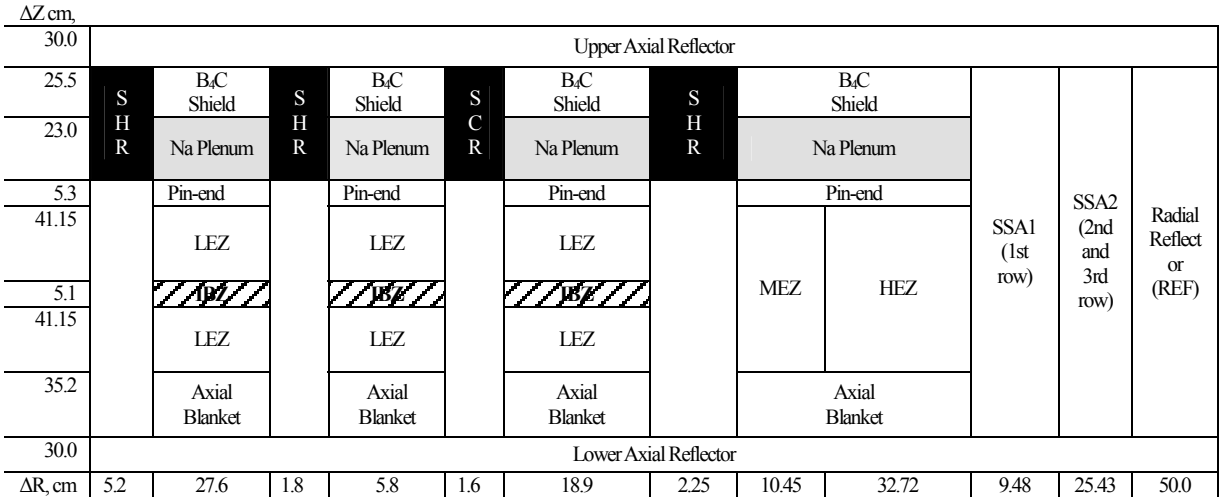

Fig.2 RZ calculational model indicating axial arrangement of compositions

The RZ calculational model indicating the axial arrangement of compositions is shown in Fig. 2. Several design modifications have been made in the full MOX core model, compared with the hybrid core model. A sodium plenum followed by a boron shield is located above the core to reduce the sodium void effect. An internal breeding zone (IBZ) of 5.1 cm thickness is inserted in the core mid plane to achieve the reduction of sodium void effect as sought in the BN-800 core design investigations. To compensate for the reduction in core volume resulting from these design changes, an extra row of FSAs is added in the MEZ region.

The effective multiplication factor (k_{eff}), and the integral value and/or its spatial distribution of seven parameters including kinetics parameters were calculated by diffusion theory with the same definitions as in the previous benchmark studies, using homogeneous representations of the material regions in HEX-Z geometry. Where possible, first order perturbation theory based on heterogeneous geometry diffusion/transport theory was optionally used for the calculation of distributed reactivity coefficients and again, optionally, heterogeneous transport theory for integral values. Detailed heterogeneous geometry configurations were used for the core fuel regions and the control rods in the heterogeneous core model. The core power distribution was normalized to the total power of 1470 MW_{th} based on a local energy deposition model where energy is deposited at the point of fission with an energy of 200 MeV per fission and 0 MeV per capture for all nuclides.

3. Homogeneous Benchmark

The homogeneous portion of the benchmark results will be presented in three sections. The first section discusses integral reactivity coefficients and kinetics parameters, while the second section discusses local (spatially dependent) reactivity coefficients. Finally, the last section discusses power distributions.

3.1 Integral reactivity coefficients

Integral reactivity coefficients and kinetics parameters obtained by the participants are given in Table 1 with the mean values and relative standard deviation of the results for each parameter. In this table, the IPPE results obtained based on two-dimensional transport theory calculational results are given only for inter-comparison and not included in the mean value estimation. The reactivity coefficients for sodium density (W_{Na}), fuel density (W_{fuel}), steel (structure) density (W_{steel}), and Doppler effect were calculated based on the same definitions as specified in the previous benchmarks. That is, the density coefficients (material worths) for sodium, fuel and steel are defined in terms of $\partial k/k\ k'/\partial\rho/\rho$; this is the reactivity change per 1% reduction in material density. The fuel and steel Doppler coefficients (K_D^{fuel} and K_D^{steel}) were calculated for temperature changes in the fuel (1500 K to 2100 K) and structure (600 K to 900 K) respectively for a flooded core state. The comparison of the diffusion and transport results generally shows good agreement for most parameters except for the sodium density coefficient.

HEX-Z diffusion and transport theory calculations predict the k_{eff} as 1.00131 and 1.00664 with corresponding relative standard deviations of 0.60% and 0.33%, respectively. Using diffusion theory, the evaluated mean effective delayed neutron fraction is β_{eff} = 0.00341 and the prompt neutron lifetime is l_p = 4.309 x 10^{-7} sec with

standard deviations of 2.4% and 4.1%, respectively.

The fuel Doppler coefficient, one of the most important parameters in dynamic analysis, was evaluated to be –0.00737 and –0.00729 with relative standard deviations of 9.7% and 8.0% for diffusion and transport theory calculations, respectively. Deviations for the fuel Doppler coefficient from the mean value range from 20.5% (KAERI) to –11.5% (FZK/IKET). The steel Doppler was evaluated to be ~ 1/8 the magnitude of the fuel Doppler. The steel Doppler coefficient was predicted with standard deviations of 24.5% and 33.2% for diffusion and transport theory calculations, respectively. The larger dispersion in the prediction of the steel Doppler, compared with the fuel Doppler, is attributable to the sum of its smaller spatial contributions wider spread over the entire core system.

The fuel density coefficient predicted to be 0.3806 and 0.3826 with relative standard deviations of 3.1% and 1.0%, shows good agreement in diffusion and transport theory approximations. The integral sodium density coefficients are 0.00114 and –0.00150 with substantially large relative standard deviations for the diffusion and transport theory results. This is due to the fact that, by design, a small (close to zero) integral sodium density coefficient was aimed for, to achieve low or even below zero sodium void worth. Due to the close to zero value, there is a relatively large dispersion and even sign change between the diffusion theory results. If the ANL result is ignored, this change ranges from +0.00139 (0.13$) (IPPE) to –0.00199 (-0.43$) (CEA/SA). There is also a relatively large difference between the diffusion and transport theory results also with opposite signs. For the core model of the BN-600 type fast reactor including an IBZ zone and an above core sodium plenum the sodium density coefficient is significantly affected by the nuclear data set used, approximations in the calculational methods as well as the compensation between positive central terms and negative leakage terms.

3.2. Local reactivity coefficients

Distributions of local reactivity coefficients were determined using the diffusion theory based, first order perturbation method. In Fig. 3, the fuel Doppler coefficients for LEZ, that has the largest ^{238}U density in the core region, are the largest. In this figure, the comparison of regional coefficients shows better agreement than the comparison of the total coefficients summed over all regions. Fig. 4 shows the axial distribution of the fuel Doppler coefficients for three fuel zones obtained by IPPE. In Fig. 4, there can be seen to be substantial changes between physical zones of different compositions in the axial direction of each differently enriched fuel zone. Although not shown, the largest difference between the diffusion and transport theory results is obtained in the upper core region adjacent to the sodium plenum.

Regionwise sodium density coefficients over the whole core system are shown in Figs. 5 split into leakage and non-leakage components along with the average values. In these figures, the first six groups of columns (LEZ, MEZ, HEZ, IBZ, AB and Sum) and the next four groups (SP, UBS, C&P and AR) denote the corresponding values for fuelled and non-fuelled regions in the core, respectively. The group of columns labelled by SUM denotes the total values for the core. The resultant sodium density coefficients clearly show spatial distributions that can mainly be characterized by the leakage and non-leakage components. The prevailing non-leakage component in LEZ and MEZ near the core centre becomes smaller moving toward the outer zones. It is clearly seen that the leakage component becomes dominant in the HEZ region and, as a result, the HEZ region has a positive worth. In the HEZ region, this leakage dominating effect appeared to be valid except for the results obtained by ANL and CEA/SA. The sodium plenum (SP) has a high positive worth even with its central location in the core and, as a result, it contributes strongly to making the total sodium density coefficient positive. In these figures, the comparison of regional coefficients for the core fuelled regions shows better agreement than that of other non-fuelled regions. Also the total coefficients, summed over all regions, show better agreement. This is due to relatively large differences in the spatial predictions for non-fuelled regions; the control regions (SCR and SHR) and other large non-fuelled regions (REF and SSA); based on a 1% reduction in the sodium density. Fig. 6 showing the IPPE result gives an example of the detailed spatial distributions of leakage and non-leakage components of the sodium density coefficient.

Calculation methods have the most significant effect on the sodium density coefficient. There are changes in the axial profile of the sodium density coefficient and (even larger changes) in its distribution in different enrichment zones, depending on the use of transport or HEX-Z diffusion calculations. For example, in the HEZ region, the difference between the results obtained by transport and diffusion HEX-Z analyses can be as high as ~50%. In general, most results were predicted within relative standard deviations of ~10% for the core and ~30 % for the whole core system, respectively. Large discrepancies are observed in the HEZ region in the fuelled core and even larger spreads in the sodium plenum and other non-fuelled regions.

Table 1. Integral reactivity and kinetics parameters

Participant	k_{eff}		K_D^{fuel}		K_D^{steel}		W_{Na}		W_{steel}		W_{fuel}		β_{eff}(pcm)	l_p (10^{-7} sec)
	Diffusion	Transport	Diffusion	Transport	Diffusion	Transport	Diffusion	Transport	Diffusion	Transport	Diffusion	Transport	Diffusion	Diffusion
ANL	1.00374		-0.00710		-0.00113		0.01355		-0.0484		0.3548		324	4.107
CEA/SA	1.00183	1.00946	-0.00789	-0.00788	-0.00124	-0.00126	-0.00199	-0.00334			0.3882	0.3788	350	4.365
CIAE	0.98834		-0.00683		-0.00072		-0.00099		-0.0177		0.3915		348	4.092
FZK/IKET	1.00254	1.00849	-0.00652	-0.00649	-0.00052	-0.00052	0.00127	-0.00045			0.3900	0.3815	334	4.130
IGCAR	1.00164		-0.0717				0.00090		-0.0185		0.3790		346	4.510
IPPE*	1.00578	1.00589	-0.00684	-0.00726	-0.00110	-0.00118	0.00139	-0.00723	-0.0126	-0.0135	0.3786	0.3782	344	4.530
JNC	0.99687	1.00196	-0.00770	-0.00750	-0.00100	-0.00100	0.00084	-0.00067	-0.0159	-0.0245	0.3908	0.3875	336	4.484
KAERI	1.00976		-0.00888		-0.00101		0.00223		-0.0041		0.3772		342	4.257
Mean	1.00131	1.0664	-0.00737	-0.00729	-0.00096	-0.00093	0.00046	-0.00149	-0.0195	-0.0245	0.3806	0.3826	341	4.309
SD (±) (Rel. %)	0.00599 (0.60)	0.00333 (0.33)	0.00071 (9.7)	0.00059 (8.0)	0.00023 (24.5)	0.00031 (33.2)	0.00480 (1052.2)	0.00131 (88.3)	0.0138 (70.4)		0.0118 (3.1)	0.0036 (0.9)	8.18 (2.4)	0.175 (4.1)

* Transport values for reactivity coefficient (RC) given by $RC^{*}_{HEX,Z} = RC^{Diff}_{HEX,Z} \dfrac{RC^{Transp}_{R,Z}}{RC^{Diff}_{R,Z}}$.

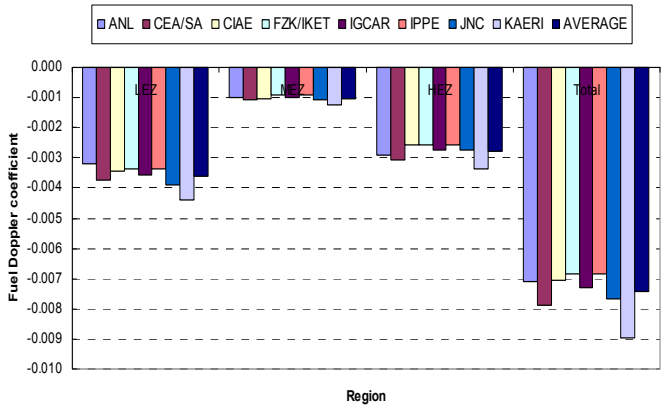

Fig. 3. Fuel Doppler coefficient

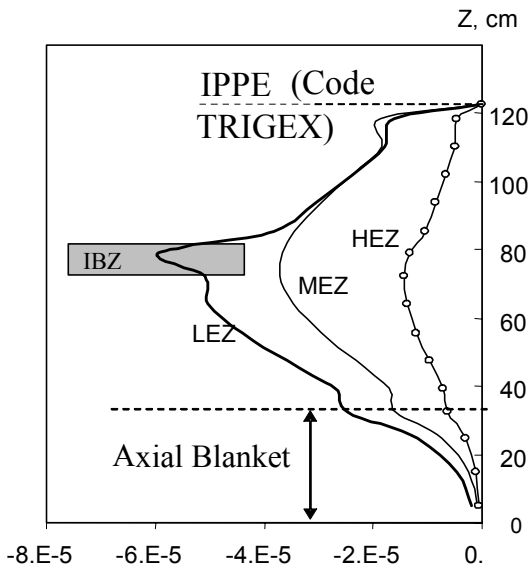

Fig. 4. Axial distribution of the fuel Doppler coefficient (for $\Delta Z = 1$ cm) (IPPE result)

For such a complicated core configuration under study, a low numbered energy groups (e.g., ~ 10 energy groups) may not be sufficient to accurately evaluate reactivity coefficients. The use of a few energy groups approximation with a uniform convolution of groups in different regions, may smooth out important spectral contributions to the reactivity coefficient. This effect will be especially important in the calculation of fuel Doppler and sodium density coefficients at the top of the core and in the sodium plenum. [6] The latter has the most important effect on the simulation of reactor dynamics, as the sodium temperature rise is at its maximum in these regions.

3.3. Power distributions

Regionwise normalised power fractions, calculated based on a local energy deposition model, are shown in Fig. 7 along with their average values. In the local energy deposition model, the contributions to the power from non-fuelled zones are completely ignored. Power fractions for enriched fuel regions, i.e., LEZ, MEZ, and HEZ, are calculated within a maximum 4.3% divergence (in the LEZ zone) from the average value, while for blanket regions, i.e., IBZ and ABZ, within a maximum 16.1% divergence in ABZ. The comparison of regionwise power distributions generally shows good agreement for the HEX-Z model. Given the local energy distribution model, approximately 96.5% of total power is produced in the enriched fuel zones and 3.5% is produced in the blanket regions. The HEZ region, which contains fuel with an enrichment of 18.5wt% with 91.3wt% ^{239}Pu content, produces 47.5% of the total power.

4. Heterogeneous Benchmark

The same reactivity parameters as in the homogeneous benchmark, were calculated using a heterogeneous treatment of the core fuel regions, axial blanket and SHR absorber region. The detailed heterogeneous geometry description and approximations to the real geometry of fuel assemblies and SHR control rods are the same as used in the previous benchmarks. [4,5] Fuel assemblies for LEZ, MEZ and HEZ have an identical geometry, in which 127 fuel pins are located on a triangular pitch of 7.95 mm inside a hexagonal wrapper. In the evaluation of the heterogeneity effect, the heterogeneous geometry of the SHR control rods has been treated in the same way as in the previous benchmarks, by employing various specific heterogeneous modeling methods with specific procedures for reaction rate preservation. [4]

Integral reactivity parameters calculated for the homogeneous and heterogeneous core models with the SHR rods at mid-core insertion are compared in Table 2. Most reactivity parameters and resultant heterogeneity effects show good agreement for diffusion and transport theory results, except for sodium density. The heterogeneity effect on k_{eff} was evaluated to be an increase of 271 pcm and 288 pcm for the diffusion and transport theory calculations,

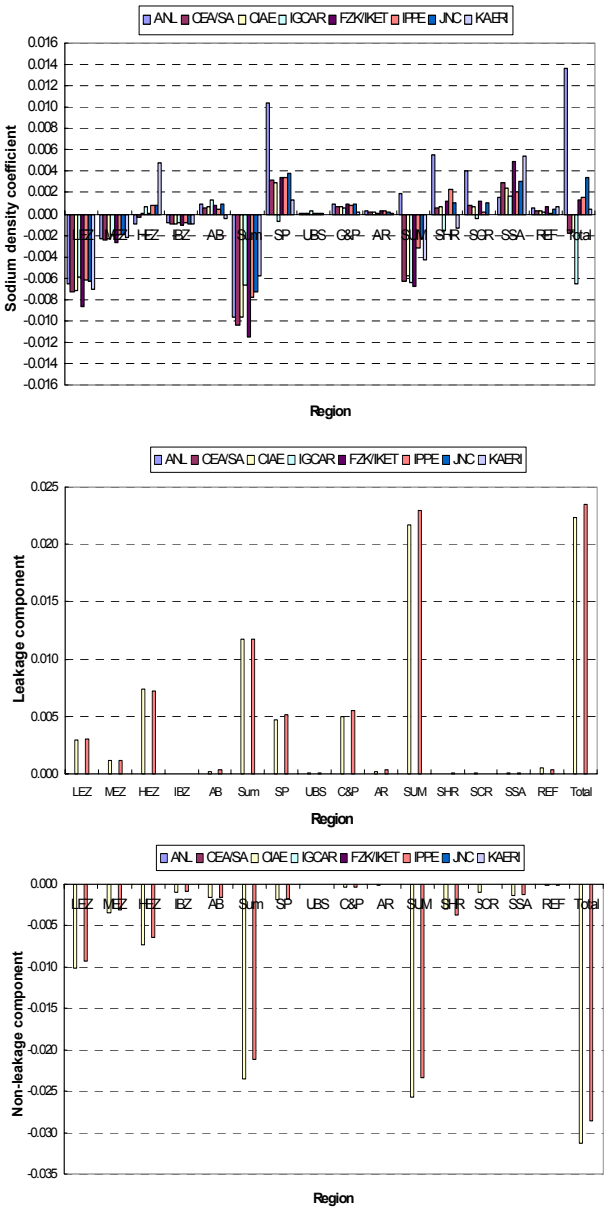

Fig. 5. Regionwise sodium density coefficients

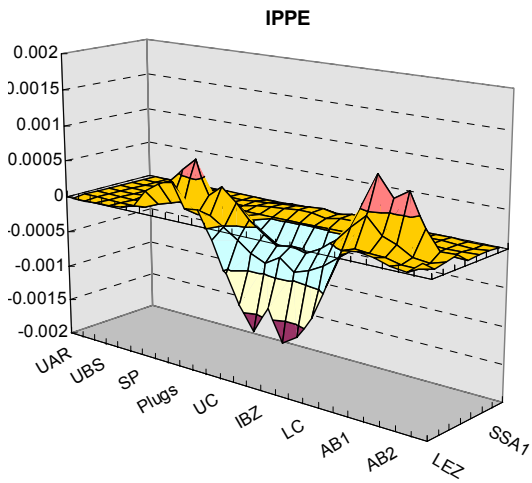

Fig. 6. Sodium density coefficient distributions (IPPE Result)

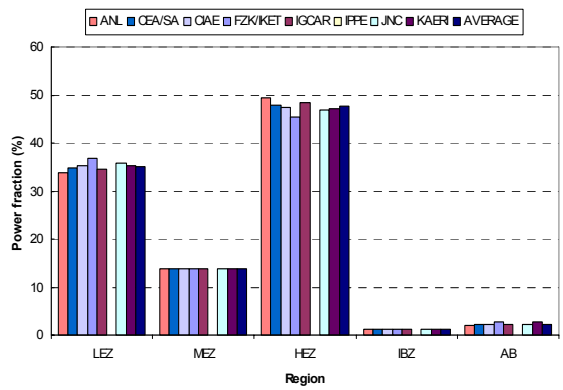

Fig. 7. Regionwise power distributions

respectively. The results appear to differ depending on the heterogeneity treatment method, similar to the previous benchmark. [4,5] The fuel Doppler coefficient becomes more negative by 5.7% and 5.2% for both approximations using a heterogeneous treatment. The heterogeneity effect on the steel Doppler coefficient appears to be negligibly small in the majority of results.

Table 2. Heterogeneity effect

Participant	k_{eff}			K_D^{fuel}			K_D^{steel}		
	Diffusion	Transport	Hete. effect (pcm)[1)]	Diffusion	Transport	Hete. effect (%)[2)]	Diffusion	Tranpsort	Hete. effect (%)
CEA/SA	1.00513 (1.00183)[3)]	1.01271 (1.00946)	329 (325)	-0.00852 (-0.00789)	-0.00850 (-0.00788)	7.97 (7.79)	-0.00120 (-0.00124)	-0.00120 (-0.00126)	-3.62 (-4.61)
CIAE	0.98974 (0.98834)		140	-0.00710 (-0.00683)		4.04	-0.00073 (-0.00072)		0.29
FZK/IKET	(1.00254)	1.01023 (1.00849)	(174)	(-0.00652)	-0.00684 (-0.00649)	(5.39)	(-0.00052)	-0.00053 (-0.00052)	(1.87)
IPPE	(1.00578)	1.01078±0.015%[4)] (1.00589±0.010%)							
JNC	1.00030 (0.99687)	1.00560 (1.00196)	343 (364)	-0.00810 (-0.00770)	-0.00770 (-0.00750)	5.19 (2.67)	-0.00810 (-0.00770)	-0.00770 (-0.00750)	-30.00 (-20.00)
Mean	0.99839	1.00951	271 (288)	-0.00755	-0.00768	5.73 (5.23)	-0.00088	-0.00084	-16.81 (-12.30)
SD (±)	0.00643	0.00295	93 (82)	0.00080	0.00068	2.02 (3.62)	0.00023	0.00028	18.66 (10.88)

Participant	W_{Na}			W_{steel}			W_{fuel}		
	Diffusion	Transport	Hete. effect (%)	Diffusion	Transport	Hete. effect (%)	Diffusion	Transport	Hete. effect (%)
CEA/SA	0.00228 (-0.00199)	-0.00039 (-0.00334)	-214.25 (-88.31)				0.3830 (0.3882)	0.3735 (0.3788)	-1.34 (-1.40)
CIAE	-0.00056 (-0.00090)		-43.20	(-0.30177)			0.3902 (0.3915)		-0.32
FZK/IKET	(0.00127)	0.00590 (-0.00045)	(-1411.11)				(0.3900)	0.3802 (0.3815)	(-0.35)
JNC	0.00410 (0.00084)	0.00040 (-0.00067)	391.02 (-159.61)	-0.0124 (-0.0159)	-0.0185 (-0.0245)	-22.21 (-24.61)	0.3754 (0.3908)	0.3698 (0.3875)	-3.94 (-4.56)
Mean	0.00194	0.00197	44.48 (-123.96)	-0.0124	-0.0185		0.3829	0.3745	-1.87 (-2.10)
SD (±)	0.00192	0.00280	312.04 (50.42)				0.0060	0.0430	1.87 (2.19)

Notes: 1) Heterogeneity effect = (Hete. – Homo.) x 10^5 (pcm) based on diffusion results, and transport results denoted by parenthesis
2) Heterogeneity effect = (Hete. – Homo.) x 100 (%) based on diffusion results, and transport results denoted by parenthesis
3) Values in parenthesis denote homogeneous results.
4) Monte Carlo results

Most heterogeneous treatment results obtained by diffusion and transport theory calculations show the increase of the sodium density coefficient. However, there remains a large standard deviation, and even an opposite sign in the heterogeneity predictions based on both approximations. The large standard deviation in the predictions is conjectured to come from the summation over very small spatial contributions from non-fuelled regions when determining the sodium density coefficient for the heterogeneous core model, as observed in the case of the homogeneous calculations. Regionwise sodium density coefficients become more positive in the heterogeneous core model calculations. This aspect holds over all core regions, and even results in a positive value relative to a negative one in the homogeneous core model calculations. Only one result calculated with the heterogeneous core model shows a decrease in the steel density coefficient. With the heterogeneous core model, the fuel density coefficient is decreased by ~ 2.0% in its magnitude for diffusion and transport theory calculations, indicating only a small heterogeneity effect. Both diffusion and transport theory calculations show good agreement in predicting the fuel density coefficients even with the heterogeneous treatment of fuel subassemblies.

Apparently the heterogeneity effect on the power distribution is negligibly small. The heterogeneous core model calculations, based on diffusion theory, increase the effective delayed neutron fraction and prompt neutron lifetime by 0.4% and 1.1%, respectively. The heterogeneity effect on these kinetic parameters appears to be small.

5. Simplified Approach to Accident Process Modeling

IPPE initially compared the reactivity coefficients provided by the participants in terms of the values of the discrepancies, and investigated their effects on the ULOF and UTOP transient behaviors of the BN-600 full MOX benchmark core in a simplified transient analyses. [6] Unavailable input data for reactivity coefficients, not provided by some participants, were taken from three-dimensional diffusion calculations using the TRIGEX code. In the previous analysis of the BN-600 hybrid core, deviations of reactivity values caused by thermal expansion of materials in radial and axial directions ranged within ~10% for both R-Z and HEX-Z geometry models regardless of calculational approximations. The reactivity balance between radial expansion and other reactivity effects showed good approximation to describe the dynamic reactivity processes compared with precise Monte Carlo calculations. [4,5] A simple model of a truncated core was used to evaluate the reactivity effect due to radial expansion. To include the reactivity contribution of the steel reflector, it was assumed that the radial steel blanket assemblies (SSAs) are incorporated into an additional thermo-hydraulics channel where reactivity effects are determined only by the sodium temperature change. For these calculations 1% of a fictitious energy release from the fuel is allocated to the SSA.

5.1. UTOP accident

In a similar way to the previous hybrid core analysis, an inadvertent withdrawal of control rod having 0.1% worth during 7.5 sec (linear input of reactivity) was assumed for the reactivity perturbation. Preliminary analysis showed that this perturbation would not result in exceeding maximum permissible temperature values. It appears that modeling uncertainties are the main source of difference in maximum temperatures, although the sums of the reactivity feedback components do not differ much (the difference in the net effect can only be large in the time interval when the total reactivity is close to zero).

Fig. 8 shows contributions of the various fuel zones to the total reactivity in the UTOP and ULOF accidents. It is concluded that, given the large contribution of LEZ, most attention should be paid to the accuracy of the calculation of reactivity coefficients in this zone, from the viewpoint of reducing modeling uncertainties.

The main conclusions resulting from the various UTOP analysis calculations include:

- Change from diffusion to transport approximation with the same RZ model causes the following divergences: ~ 17 – 20 MW for the maximum power (~1%) (the diffusion approximation predicts a higher level of power), and ~ 5 ^{o}C for sodium and ~ 15 ^{o}C for fuel for maximum temperatures;
- Change to more complicated model (from the RZ model to the HEX-Z model) with the same diffusion approximation approach results in the following divergence of the above parameters: ~60 MW for power (3.5%), 7 - 10 ^{o}C for sodium temperature and 60 - 65 ^{o}C for fuel temperature. Three-dimensional analysis predicts higher limiting parameter values.

The magnitude of the modeling uncertainty is found to be higher than that of the methodological uncertainty. These uncertainties have opposite sign. As in the previous hybrid core analyses, parameter differences seen from various calculational approximations are larger, while the maximum values of power and material temperature are lower in the UTOP accident. This demonstrates the enhancement of the inherent safety in the reactor due to the

introduction of sodium plenum above the core.

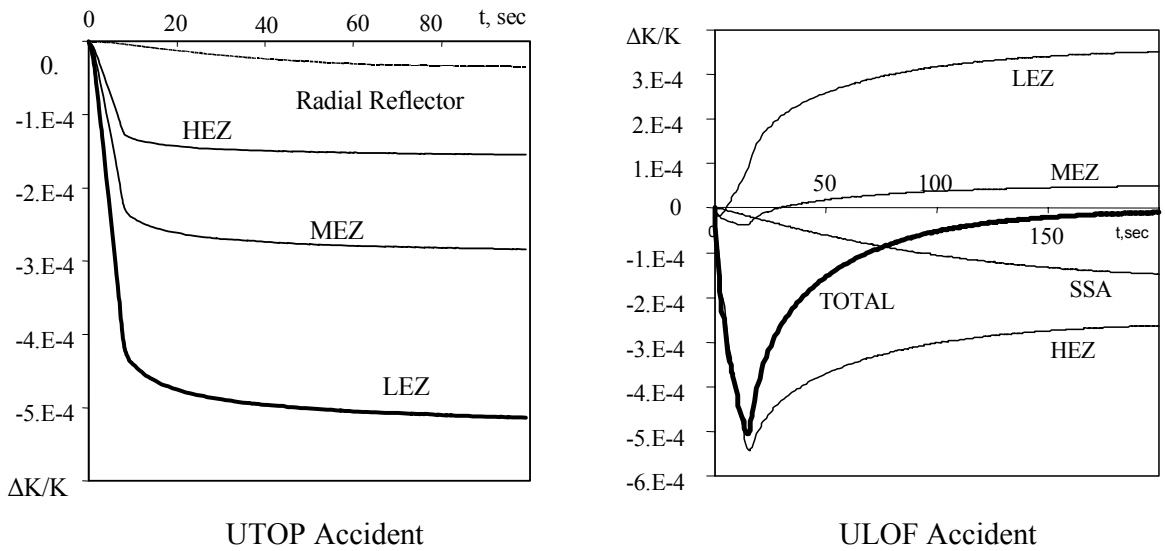

Fig. 8. Contributions of various fuel zones to total reactivity (diffusion approach, HEX-Z model)

5.2. ULOF accident

For the analysis of ULOF accident, a 30% flow rate decrease transient was considered. Figs. 9 -11 compare the results obtained from the HEX-Z diffusion calculations, provided by different participants.

Even with the same temperature history even using believable differences in reactivity coefficients results in large differences in the total reactivity feedback, with a maximum at a level ~ 40 % (see Figs.10 – 11). According to the ANL results, the large sodium density coefficient in the sodium plenum results in an increase of the negative feedback through the temperature feedback mechanism. The maximum temperature obtained with the ANL result appears to be higher than the others due to the larger positive value of the Doppler effect, especially at the bottom part of the core. Differences in key parameters in the ULOF accident, due to the differences in calculated values for sodium density reactivity coefficient, especially the large (maximum) differences in the sodium plenum, produce resulting differences of ~60 MW for power, > 100 °C and ~35 °C for the maximum temperatures for the fuel and sodium, respectively.

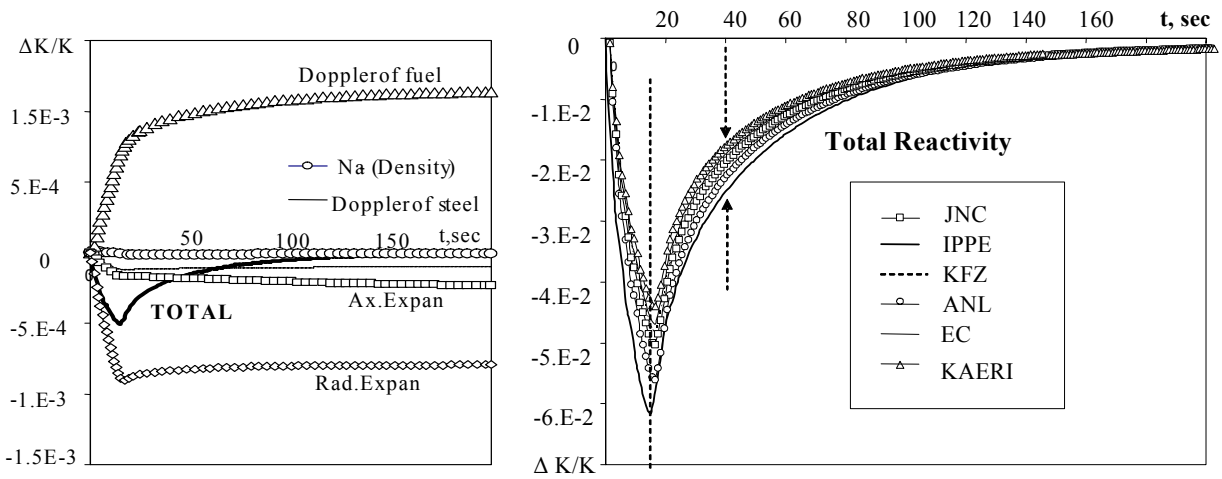

Fig. 9. Contributions of reactivity components to total reactivity in ULOF accident (diffusion approach for the reactivity parameters, HEX-Z model)

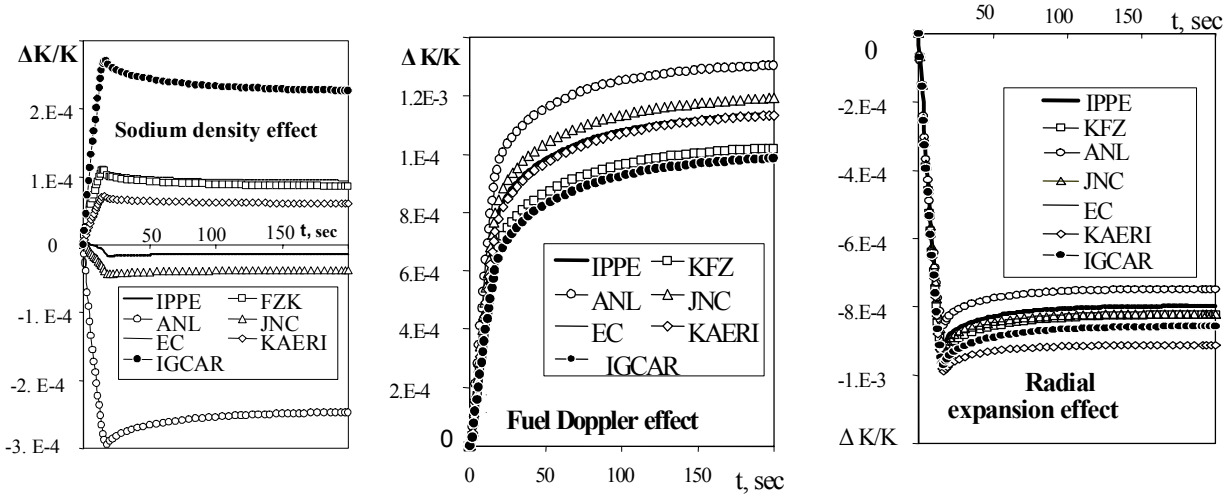

Fig. 10. Change of basic feedback reactivity components in ULOF accident

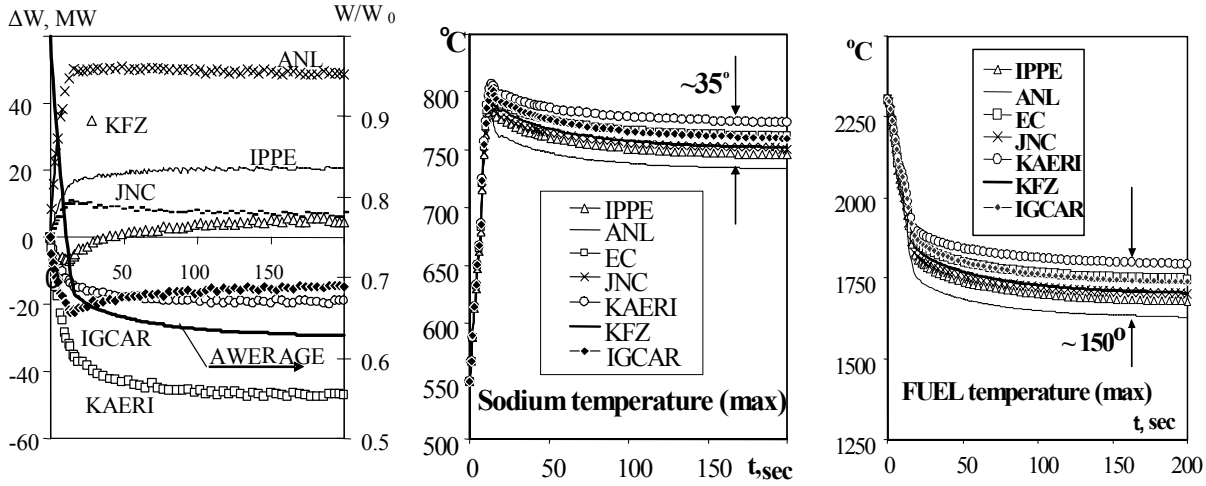

Fig. 11. Change of power and basic temperatures in ULOF accident

Fig. 12 illustrates the differences resulting from evaluations using the diffusion and transport approximation and those resulting from the inclusion of heterogeneous corrections to the description of the ULOF accident. These results were calculated based on the FZK/IKET results. Diffusion calculations in general predict a smaller value of a negative total feedback reactivity which results due to a smaller positive Doppler effect. Calculations using the reactivity coefficients obtained using the transport approximation predict higher limiting temperatures. This indicates that using the transport approximation for the determination of reactivity coefficients, leads to the prediction of more hazardous conditions for the ULOF accident and less hazardous conditions for the UTOP accident.

It is concluded that uncertainties in the model geometry are dominant over those of methodology in the description of accidents in benchmarks for the hybrid core and for the full MOX core as well. [1,5] That is, differences between maximum parameter values are lower for HEX-Z geometry than that for RZ geometry. The account of heterogeneous structure reduces discrepancies between diffusion and transport results in this study. The results also show that the heterogeneity effect evaluated using the diffusion approximation does not have any significant effect on the description of the transient behaviour.

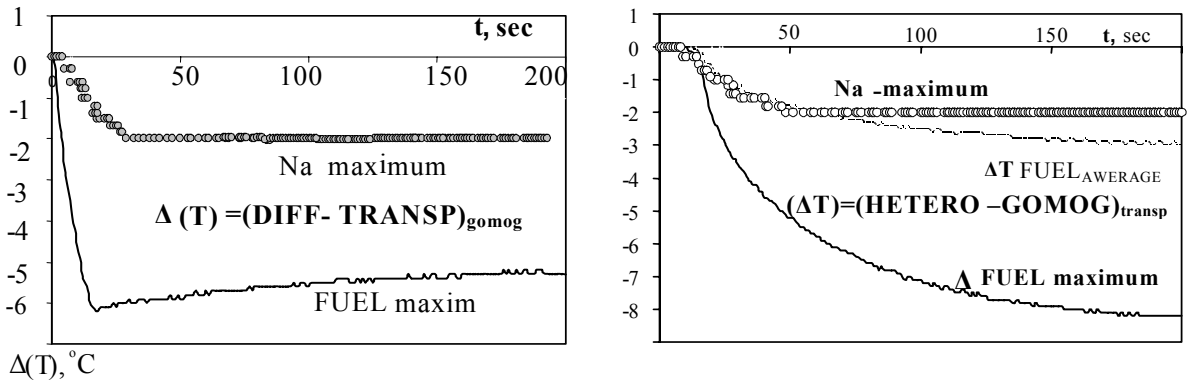

Fig. 12. Influence of transition from diffusion to transport approach and heterogeneous corrections to the description of ULOF accident (based on the FZK/IKET result)

The possible influence, due to the accuracy of power distributions calculations, was investigated by using an averaged power profile obtained with the participants' data. The analysis results using data from FZK/IKET and JNC showed an insignificant influence due to calculated differences on the prediction of power distributions. The presence of a fertile zone (IBZ) deforms the axial distribution of the fuel Doppler effect under accident conditions, but rather small differences in the fuel Doppler effect between axial layers are enhanced due to temperature changes. Differences in the sodium density effect result from the accuracy of the calculation of the sodium density coefficient in the sodium plenum where the coolant temperature is a maximum.

Differences in reactivity effects due to the thermal expansion of materials (both axial and radial) are insignificant, similar to the case of the previous hybrid core model.

For the benchmark considered, calculational uncertainties in basic reactivity coefficients result in the following differences in the maximum temperatures:

	Power	Max. sodium temperature	Max. fuel temperature
- Uncertainty of sodium density coefficient	< 20 MW	20 °C	50 °C
- Uncertainty of fuel Doppler coefficient	< 10 MW	10 °C	< 30 °C
- Uncertainty of material expansion coefficient (max → 0)	~ 150 MW	~ 150 °C	~ 300 °C

6. Conclusions

The comparison of the diffusion and transport results for integral and local values, generally shows good agreement between most parameters except for the sodium density coefficient. However, differences between the values of the main reactivity coefficients obtained by the participants, appear to be larger in the reference model (BN-600 full MOX core model) than those obtained in the previous model, with a traditional core arrangement (BN-600 hybrid core model). This arises mainly because of uncertainties in the proper modelling of the axial sodium plenum above the core. This observation relates to both the integral values and the spatial distribution of reactivity coefficients.

For the full MOX core, the choice of a low number of neutron energy groups may become critical in achieving an accurate evaluation of reactivity coefficients. This applies mainly the fuel Doppler coefficient and the sodium density coefficient at the top of the core and in the sodium plenum. The latter has the largest effect on the description of reactor dynamics, because the sodium temperature rise is maximum in these areas.

The larger differences in the spatial distribution of the reactivity coefficients has a larger effect on the prediction of maximum parameters of the UTOP and ULOF accidents in the full MOX core in comparison to the hybrid core configuration. The uncertainties introduced by modelling approximations (RZ, HEX-Z) has more influence than the choice of heterogeneous/homogeneous geometry or diffusion/transport theory. Moreover, the use of more accurate approximations than homogeneous diffusion theory is partly compensated by using a more complex geometry. The use of the diffusion theory approximation generally gives more benign consequences for the ULOF

accident, while the opposite is true for the UTOP accident in comparison with transport theory results. The results of ULOF accident analyses made with different sets of Doppler and sodium density coefficients show a considerable spread in the maximum temperature values, namely: ~ 40°C for the sodium temperature and over 100°C for the fuel temperature. The spread in the evaluated core power distribution has a minimal effect on the maximum values of ULOF accident parameters. Nevertheless, depending on the initial power, the maximum temperature may appear in different core regions. The spread in calculated reactivity effects due to the thermal expansion of materials (both axial and radial) is insignificant, similar to the case of the previous hybrid core model analysis. Detailed heterogeneity effects do not have any significant effect on the description of the accident process.

References

1) IAEA, "Working Material: Updated Codes and Methods to Reduce the Calculational Uncertainties of the LMFR Reactivity Effects, The fourth Research Co-ordination Meeting," Obninsk, 19-23 May 2003, IAEA-RC-803.4, TWG-FR/113 (2003).
2) IAEA, "Working Material: Updated Codes and Methods to Reduce the Calculational Uncertainties of the LMFR Reactivity Effects, The first Research Co-ordination Meeting," Vienna, 24-26 November 1999, IAEA-RC-803, IWG-FR/100 (2000).
3) IAEA, "Working Material: Updated Codes and Methods to Reduce the Calculational Uncertainties of the LMFR Reactivity Effects, The second Research Co-ordination Meeting," Vienna, 24-26 November 2000, IAEA-RC-803.2, IWG-FR/103 (2000).
4) IAEA, "Working Material: Updated Codes and Methods to Reduce the Calculational Uncertainties of the LMFR Reactivity Effects, The third Research Co-ordination Meeting," Cadarache, 12-16 November 2001, IAEA-RC-803.3, TWG-FR/106 (2001).
5) Y. I. Kim, et al., "BN-600 Hybrid Core Benchmark Analyses," *Proc. of the PHYSOR 2002*, Seoul, Korea, October 7-10, 2002, ANS (2002).
6) A. Danilytchev, D. Elistratov and V. Stogov, "Reactivity Coefficients and Simplified Approach to Accidents Process Modeling (Phase 4)," IAEA-RC-803.4, TWG-FR/113 (2003).